crystals

Erschienen in: Crystals ; 7 (2017), 7. - 207
http://dx.doi.org/10.3390/cryst7070207

MDPI

Review

Mesocrystals: Past, Presence, Future

Elena V. Sturm (née Rosseeva) * and Helmut Cölfen *

Physical Chemistry, Department of Chemistry, University of Konstanz, Universitätsstr. 10, D-78457 Konstanz, Germany

* Correspondence: elena.sturm@uni-konstanz.de (E.V.S.); helmut.coelfen@uni-konstanz.de (H.C.); Tel.: +49-7531-88-4063 (H.C.)

Academic Editor: Monica Distaso
Received: 15 June 2017; Accepted: 4 July 2017; Published: 9 July 2017

Abstract: In this review, we briefly summarize the history of mesocrystal research. We introduce the current structural definition of mesocrystals and discuss the appropriate base for the classification of mesocrystals and their relations with other classes of solid state materials in terms of their structure. Building up on this, we comment on the problems in mesocrystal research both fundamental and methodological. Additionally, we make the short overview of the mesocrystal formation principles and synthetic routes used for their fabrications. As an outlook into the future, we highlight the most notable trends in mesocrystal research and developments.

Keywords: mesocrystal; nanostructured materials; structure; self-assembly; synthesis; collective properties

1. Introduction and Brief Historical Remarks

Around 10 years ago the term mesocrystal (i.e., mesoscopically structured crystalline materials) was proposed to define superstructures of nanocrystals with a common crystallographic orientation [1–4]. The term mesocrystal had already been used before in earlier reports, but usually in reference to crystalline materials of mesoscopic size or of mesoporous structure [5–9]. Although it might seem from Figure 1 that mesocrystals are a quite recent development and discovery, the structures which are nowadays referred to as mesocrystals were already known for quite a long time.

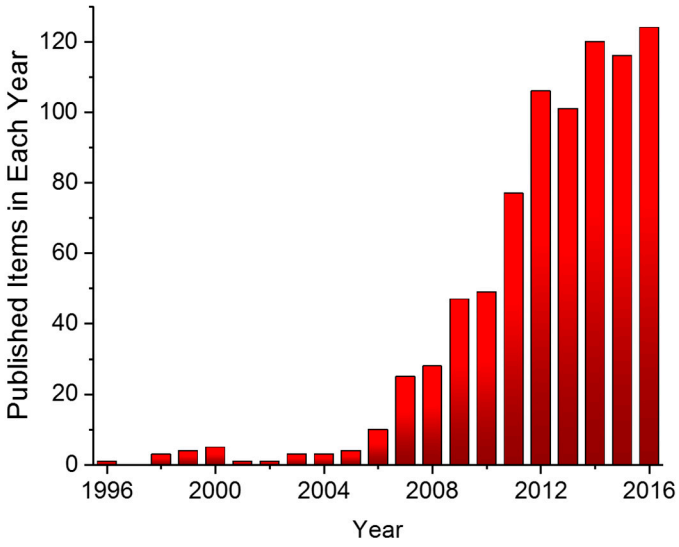

Figure 1. Papers published per year on mesocrystals as found by the search words "mesocrystal*" in the Web of Science by the end of 2016.

Historically, the interest in such materials has always been associated with the description of defected structures and formation mechanisms of natural minerals and their synthetic analogues [10–12]. As an example, Figure 2a,b illustrates the particle mediated crystal growth mechanism proposed by Shubnikov (in 1933, 1935) [10,13] and Yushkin (in 1971) [14], based on an investigation of potassium alum and sulfur aggregates. Back then, several terms were already proposed to describe such structures (including mosaic crystals, block-like crystals, pseudo-single crystals (pseudomonocrystals) etc. [11,12,14–19]). Furthermore, a great development in this area has been made due to the investigation of colloidal aggregates and periodic colloidal structures [20–25]. In the earliest reports dating back to 1925, Blüh described the oriented aggregation of rod-like V_2O_5 particles on a glass surface [26], while Zocher and Heller (later with co-workers) examined so-called "Schiller layers" or "Tactoids" (prepared from colloidal solutions of iron oxides and/or iron (oxi-)hydroxides) [10,27–31]. Another interesting early report described the oriented aggregation of PbSe cuboctahedrally shaped particles on a silicon surface (Figure 2c); this approach was used to examine the distribution of active centers on the surface of catalytic materials [32]. However, due to the limited analytical possibilities at that time, all of these structures could not be analyzed with the necessary rigor. More about early reports on mesocrystals (and related crystalline materials) can be found in chapter 7.2 of Ref. [4].

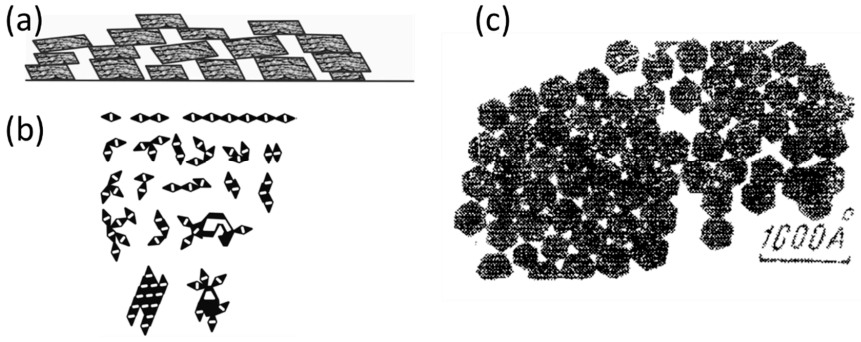

Figure 2. Examples of early reports on the formation of "block-like" and/or "mosaic" crystals and self-assemblies of nanocrystals with mutual orientation. (**a**) Schematic illustration of particle mediated growth of crystals via oriented attachment of submicron-sized building blocks (Shubnikov scheme: based on experimental observation of growth process of potassium alum crystals) [10,13]. (**b**) Schematic illustration of oriented assembly of colloidal sulfur particles in solution (according to the Yushkin model) [14]. (**c**) Electron microscopy image of self-assembled PbSe particles on a Si substrate. Cuboctahedrally shaped nanoparticles assembled in close-packed monolayers and oriented with mainly {111} faces parallel to the substrate [32].

Although the structure, formation mechanism and properties of nanocrystal superstructures, mosaic crystals and other nanostructured materials have already been investigated for several decades, the dedicated and systematic research on mesocrystals (which are a special type of nanostructured materials) only started about 10 years ago. Since then, based on the analysis of structure and formation principles of mesocrystaline materials of different origin (including natural biominerals and minerals as well as synthetic materials (Figure 3)), the classification of mesocrystals has become clearly defined and their structural relations to other classes of solid state materials have been established [33,34]. It is very interesting to note that nature also applies mesocrystal structures in biominerals (Figure 3), likely to improve their mechanical properties [33]. Examples are sea urchin spines [35], nacre [36], corals [37–40] or egg shells [41]. This demonstrates that the hybrid architecture of mesocrystals obviously has some evolutionary advantages. Furthermore, it is also important to mention, that the area of application has been explored and many successful examples for improved performance by mesocrystals compared to existing technology have been reported, especially in the highly competitive area of energy storage materials [42–45]. On the other hand, very little is still known about mesocrystal

formation processes, which are, however, fundamental for the understanding of how a mesocrystal structure can be synthesized and how the synthesis can be controlled. The reasons can be found in the limited analytical capabilities, as mesocrystal formation occurs over several time and length scales. Starting with nanoparticle formation on the length scale of a few nm, up to the size of the final mesocrystal in the range of tens or hundreds of micrometers or even bigger, this range covers about 5 orders of magnitude, which is certainly a challenge for each analytical technique, especially considering that the analysis should preferably be performed in a solution. Looking at the involved timescales, the range is even larger. Primary particle formation takes place on the sub-ms time scale [46,47] and the final mesocrystal formation and structural ripening occurs on the time scale of hours or even days. Therefore, the time scale range of interest in mesocrystal formation is extremely broad, spanning up to 8 orders of magnitude (10^{-3}–10^{5} s). Thus, it becomes clear that only a combination of several analytical techniques, which work at different length and time scales, is able to reveal the structure of mesocrystals and their mechanism of formation. Suitable analytical techniques are Transmission Electron Microscopy (TEM), Scanning Electron Microscopy (SEM), Environmental Scanning Electron Microscopy (ESEM), Light Microscopy (LM), Atomic-Force Microscopy (AFM), Small-Angle X-ray Scattering (SAXS), Wide-Angle X-ray Scattering (WAXS), Small Angle Neutron Scattering (SANS), Dynamic Light Scattering (DLS), Analytic Ultra-Centrifugation (AUC) and Asymmetrical Flow Field-Flow Fractionation (AF4) to identify the different species at the different size and time scales (for a more detailed description of these techniques, see chapter 9 in Ref. [4]).

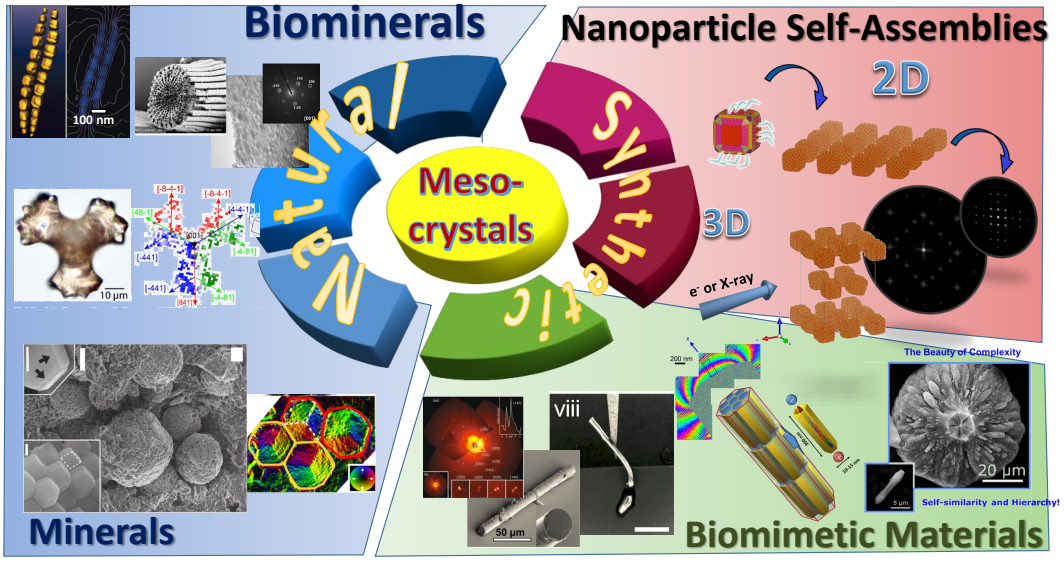

Figure 3. Schematic illustration of mesocrystals in biominerals, abiogenic minerals, biomimetic composite materials and nanoparticle self-assemblies with their structural features and physical properties. Images corresponding to biominerals: magnetite based magnetotactic bacteria are reprinted with permission from Thomas et al. (Ref. [48]), American Chemical Society; calcite based see urchin spine is reprinted from Seto et al. (Ref. [35]) and reprinted with permission of the National Academy of Sciences USA; calcite based red coral are reprinted from Floquet and Vielzeuf (Ref. [40]) with permission of ACS Publications. Abiogenic minerals: magnetite framboids from the Tagish Lake meteorite are reproduced from Ref. [49] with permission of Macmillan Publishers Limited. Colloidal self-assemblies: 2D and 3D self-assemblies of magnetite nanoparticles stabilized by oleic acid adopted from Brunner et al. Ref. [50] with permission of WILEY-VCH Verlag GmbH & Co. KGaA, Weinheim. Biomimetic materials: fluoroapatite-gelatine nanocomposites are reproduced from Ref. [51] with kind permission from WILEY-VCH Verlag GmbH & Co. KGaA, Weinheim and from Ref. [52] with permission of Springer Science and Business Media Springer-Verlag Berlin; calcite spicules are reprinted from Natalio et al. (Ref. [53]) with permission from AAAS.

Mesocrystal structures, formation mechanisms and synthesis, we have already partially discussed in several recent review articles and one book, well summarizing the previous research. Therefore, first of all, we also recommend that readers give their attention to the following Refs. [2–4,33,34,54–60]. Nevertheless, the purpose of this review is to give a short summary on mesocrystal research, including the description of their structural features, formation principles and several synthetic routes of fabrication, as well as some physical properties and related ways of application. Additionally, we take a brief look at the notable trends in mesocrystal research and development.

2. Current Status: What Is Known about Mesocrystals?

2.1. Structural Principles

The term mesocrystal was first proposed as an abbreviation for "mesoscopically structured crystalline materials", which is a special type of colloidal solid (incl. colloidal crystals) consisting of nanocrystalline building blocks with mutual alignment [2,4]. In cases where the material contains more than one phase, it can also be defined as mosaic dominated nanocomposite superstructure [51]. In accordance with the modern definition [33,34], a mesocrystal is delineated as a nanostructured material showing clear evidence that it consists of individual nanoparticle building units with a defined order on the atomic scale in at least one direction, which can be inferred from the existence of an essentially sharp wide angle diffraction pattern (although there are a number of defects interrupting the long-range order, leading to the formation of a mosaic structure of the solid). Figure 4 illustrates the classification of mesocrystals and shows their structural relationship (similarities and differences) to different classes of crystalline materials.

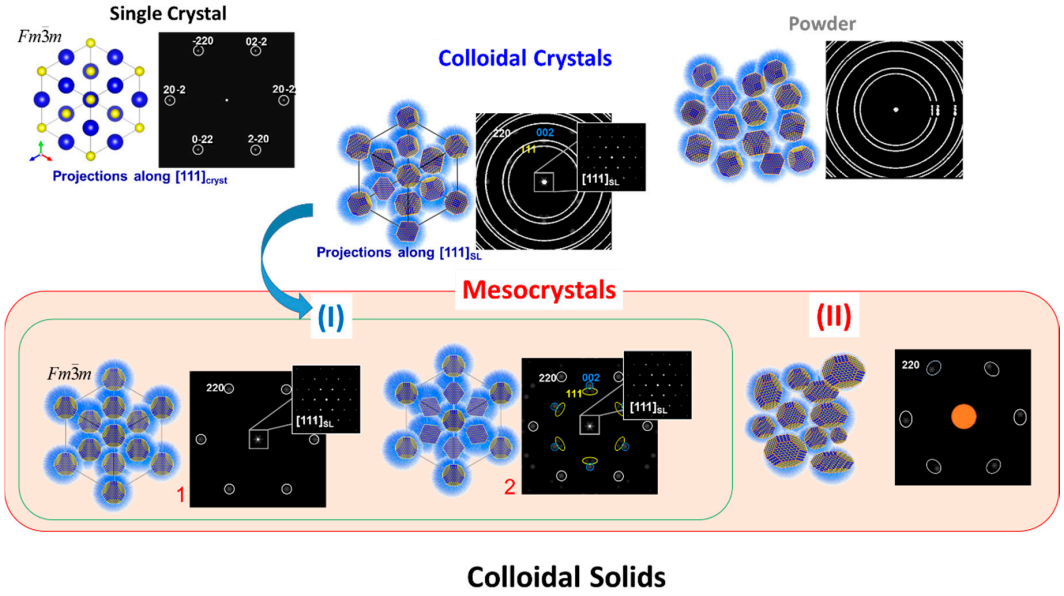

Figure 4. Schematic illustration of different types of crystalline materials with the corresponding diffraction patterns. For illustrational purposes the crystalline material (nanoparticles) has rock salt type crystal structure (S.G. *Fm*-3*m*) and in case of colloidal crystals the crystalline nanoparticles are stabilized by organic molecules (blue shell) and arranged in a face-centered cubic (*fcc*) superlattice (S.G. *Fm*-3*m*). (**Top row**) Single crystal, disordered colloidal aggregates e.g., "powder", colloidal crystal with the corresponding diffraction patterns. (**Bottom row**) Mesocrystals (red frame): type I (green frame)—colloidal crystals with mutually oriented monodisperse nanocrystals (characterized by a single crystal-like diffraction pattern in the small angle region and a single crystalline (1) or texture-like (2) pattern in the wide angle region); type II—colloidal aggregates with mutually oriented polydispersed nanocrystals with a possible certain degree of orientational mismatch.

Like a single crystal, a mesocrystal might show sharp Bragg peaks in the wide angle diffraction pattern (in contrast to the ring-like pattern for a powder), but the important difference is that a mesocrystal consists of individual nanoparticles. This is sometimes difficult to demonstrate using only the diffraction techniques (e.g., X-ray or electron diffraction) if, in the most general case, the mesocrystal building units are not monodispersed and are not arranged in an ordered superlattice array. These so-called type II mesocrystals do not show a small angle pattern with sharp diffraction peaks, which is typical of the so-called type I mesocrystals, consisting of monodisperse building units arranged in an array with long-range order (i.e., colloidal crystals). In such cases, the presence of individual nanocrystal building blocks needs to be proven by another method, e.g., electron microscopy. The difference between type I and type II mesocrystals is, therefore, the presence of nanoparticle building blocks arranged in a long-range ordered superlattice (type I), which can be evidenced by small angle diffraction techniques (e.g., SAXS, electron diffraction, etc.) (Figure 4). It may also be that the nanoparticle orientations are ordered, but they are not identical, so that a texture-like wide angle diffraction pattern results. In such cases, it is very essential to determine all crystallographic orientations which contribute to the mesocrystalline structure, as well as to define the structural principles (and/or rules) controlling and determining this specific orientational order of building blocks in the mesocrystal. Such interesting examples have already been described for several synthetic and natural systems including nanoparticles self-assemblies [50,61,62] and biominerals (i.e., red corals [38,40]). Therefore, the proof of crystalline order using the wide angle diffraction pattern together with evidence that the material consists of individual building blocks are necessary requirements to classify a solid state material as mesocrystal. The difficulties and challenges to perform in situ analysis during the formation of mesocrystals are still the main reason why mesocrystal formation mechanisms are largely unknown (since it is often concluded from the end product of the formation process, and at best, dependent on how samples were analyzed). Great potential to solve this problem is shown by recently developed in situ techniques—especially high-resolution synchrotron-based small/wide-angle X-ray scattering (SAXS/WAXS) (including in situ time-resolved grazing incidence small-angle X-ray scattering (GISAXS) and grazing incidence wide-angle X-ray scattering (GIWAXS)), as well as in situ TEM with a liquid cell. DeYoreo and colleagues have successfully observed an oriented attachment mechanism of iron oxide nanoparticles in high resolution TEM mode yielding so far unsurpassed insight into a nonclassical crystallization reaction [63–65]. Using the combination of SAXS/WAXS techniques, Wang with colleagues have already solved a number of structures of nanoparticle self-assemblies (with mesocrystalline order) [66–69]. A similar approach was introduced earlier by applying the combination of different electron microscopy techniques [50,61,62]. Bergström with co-workers examined and revealed the mechanisms of iron oxide nanoparticle self-assemblies by means of in situ GISAXS [70–75], while recently the group of W.A. Tisdale performed simultaneous in situ SAXS/WAXS measurements, revealing the kinetic rate of the self-assembly process of PbS nanoparticles; they also tracked the structural evolution of assemblies (including translational and orientational order of nanoparticles) during the formation of a mesocrystal (Figure 5) [76].

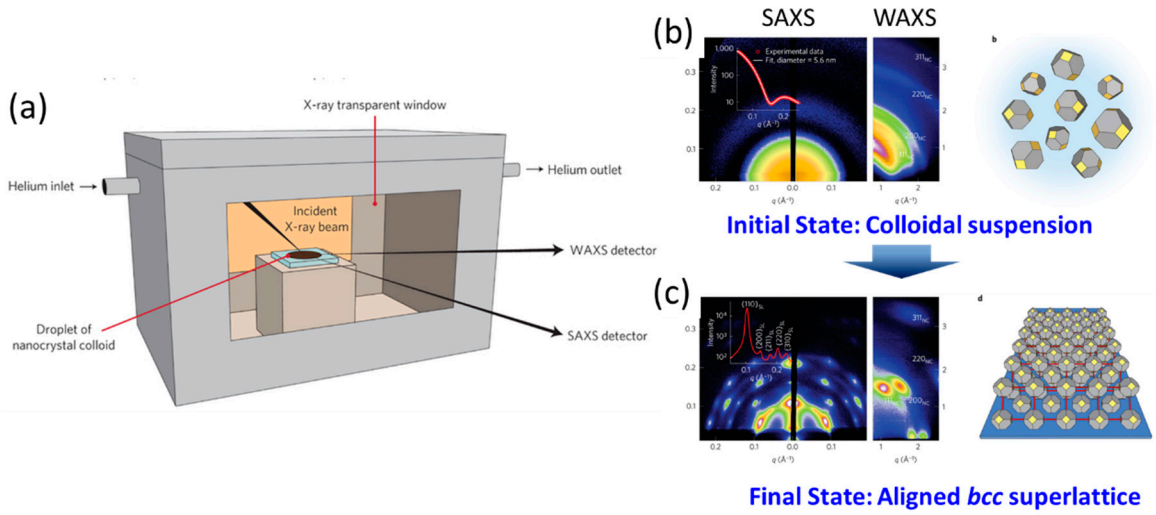

Figure 5. (**a**) Experimental set-up for simultaneous grazing incidence small-angle X-ray scattering (GISAXS) and grazing incidence wide-angle X-ray scattering (GIWAXS) measurements used for the in-situ investigation of the nanoparticle self-assembly process from dispersion by controlled solvent evaporation (**b**) and (**c**) are a short summary on experimental data (GISAXS and GIWAX patterns) and results of structural analyses showing the transformation of a disordered PbS nanoparticle dispersion to a highly ordered self-assembled *bcc* superlattice with crystallographically aligned nanocrystals (so-called mesocrystalline films). Figures are adapted from Ref. [76] with permission of the Macmillan Publishers Limited.

These techniques have rapidly been developing in recent years, and therefore, the highly desired mechanistic insight into mesocrystal formation processes might be possible to achieve in the near future. Nevertheless, the research on mesocrystals is currently being driven, not only by fundamental research, but also by application questions. Both directions are clearly interdependent, and therefore, many exciting insights into mesocrystalline systems and their physical and chemical properties are to be expected.

It is also important to mention that the specific structural order in mesocrystals might be controlled and determined not only by structural anisotropy of building blocks, including shape (Figure 6: shape control), but also by their anisotropic physical properties (Figure 6: functional control). In Figure 6 mesocrystals formed by self-assembly of magnetite nanoparticles with different size and shape are shown as an example to illustrate this phenomenon. In the case of ferrimagnetic magnetite nanoparticles, the assembly process is mainly controlled by magnetostatic dipole–dipole interactions between nanoparticles. Magnetotactic bacteria are an excellent example of a biological system exhibiting chain-like assembly of magnetite nanoparticles (magnetosomes), which functions as a magnetic sensor of direction. The magnetization direction of the single magnetite particle closes to a ⟨111⟩ crystallographic direction (which is consistent with the magnetic easy axis of magnetite). Therefore, within 1D self-assembly, magnetite nanocrystals are aligned with their ⟨111⟩ axes parallel to the chain elongation (Figure 6 blue frame, corresponding to mesocrystal Type II in Figure 4). Furthermore, electron holography data indicates the nature of the magnetic field lines similar to the dipole field lines of a rod-shaped magnet originated from the 1D directional assembly of magnetite particles [48,77].

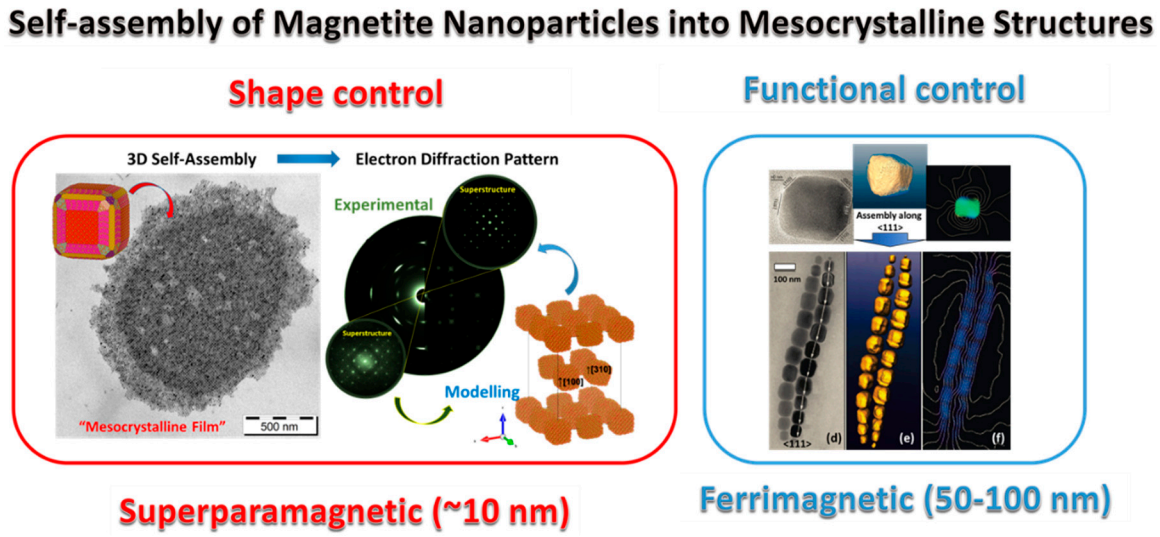

Figure 6. Schematic illustration of two main factors (driving forces) of determining the ordering of magnetite nanoparticles within mescorystalline self-assemblies. Shape Control: The small superparamagnetic nanoparticles (red frame) assembled in ordered superlattices in a way that their translational and orienational order was mainly determined by their effective shape. Figures are adapted from Ref. [50] with permission of the WILEY-VCH Verlag GmbH & Co. KGaA, Weinheim. Functional control: The ferrimagnetic magnetite nanoparticles of magnetotactic bacteria are arranged in a chain like structure and aligned along their magnetic easy axis (which corresponds to ⟨111⟩ of magnetite). Figures are adapted from Ref. [48] with permission of the American Chemical Society.

In contrast to this example, small superparamagnetic monodisperse magnetite nanoparticles can be easily assembled in 2D and 3D arrays (mesocrysals) with defined translational and orientational order (Figure 6, red frame). Our recent example [50] includes the structural investigation (by means of combination of different electron microscopy techniques) of 2D and 3D mesocrystalline film built up by 10 nm sized superparamagnetic magnetite nanoparticles stabilized by oleic acid. The magnetite nanocrystals have a cubic shape only slightly truncated by the {111}, {110}, {310} and {114} faces and can be easily self-assembled in 2D and 3D mesocrystalline films by controlled slow evaporation of solvent from the nanoparticle dispersion. In the 2D case, two distinct superlattices (SL) of magnetite nanocubes can be observed with p4mm and *c*2*mm* layer symmetries while maintaining the same orientational order with $[100]_{\text{magnetite}}$ perpendicular to the substrate (corresponding to mesocrystal Type I(1)), Figure 4). The 3D structure, which formed at the next stage of the self-assembly process, can be approximated by a *fcc* superlattice (SL). The most efficient space filling within this 3D superstructure is achieved by changing the orientational order of the nanoparticles and following the "bump-to-hollow" packing principle. Namely orientational order is determined by the shape of the nanoparticles with the following orientational relations: $[001]_{\text{SL}} \,||\, [310]_{\text{magnetite}}$, $[001]_{\text{SL}} \,||\, [301]_{\text{magnetite}}$, $[001]_{\text{SL}} \,||\, [100]_{\text{magnetite}}$ (corresponding to mesocrystal Type I(2)), Figure 4). The atomistic modelling not only verifies the proposed mesocrystal structures, but also provides great insight into fundamental principles of structuring of 2D and 3D magnetite mesocrystals. Interestingly, highly ordered magnetite based nanoparticle self-assembles can also be found in nature. The so-called framboids [49,78,79] represent a very fascinating example of natural minerals which sometimes can be classified as mesocrystals. Framboids are defined as natural colloidal aggregates or even colloidal crystals. These minerals, which often have a sedimentary origin, are usually composed of iron sulfides (e.g., pyrite) or iron oxides (e.g., magnetite) nano-/micro-crystals which can have a different degree of packing order within the aggregates. Interestingly, these materials do not even explicitly need to be of terrestrial origin. Recently, Kimura and colleagues reported on highly ordered magnetite based framboids found in the Tagish Lake meteorite (Figure 7) [49].

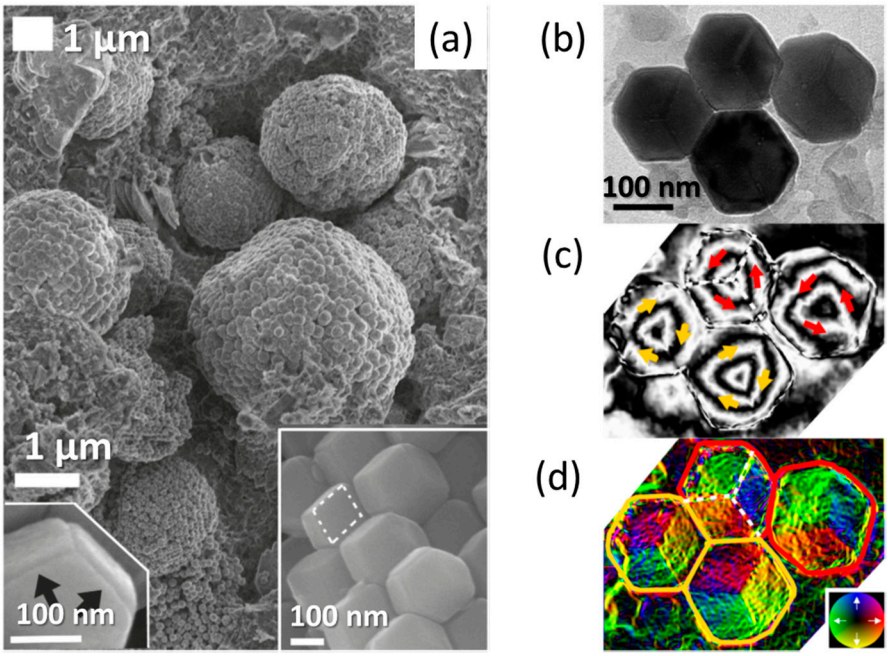

Figure 7. A short summary on the experimental observation of colloidal crystals (mesocrystals) of magnetite in the Tagish Lake meteorite. (**a**) SEM images of framboids built up by monodisperse magnetite rhombic–dodecahedraly shaped nanoparticles (bottom insets) arranged in a close-packed array with face-centered cubic (*fcc*) symmetry. (**b**) TEM image of individual magnetite nanoparticles, (**c**,**d**) reconstructed phase images obtained from the electron hologram show that each individual crystal has a vortex magnetic structure. (**d**) Color-coded magnetic induction map obtained from the gradient of the magnetic phase image. The color wheel indicates the direction of the magnetic induction. Figures are adapted from Ref. [49] with permission of Macmillan Publishers Limited.

The examined aggregates are built up by rhombic dodecahedrally shaped magnetite nanoparticles (110–680 nm) arranged in an face-centered cubic (*fcc*) superlattice (Figure 7a,b). Since, the rhombic dodecahedron is a space-filling polyhedron of the *fcc* lattice, it is quite obvious that all nanocrystals should have the same orientation within the *fcc* superlattice (Figure 7a,b). Moreover, the crystallographic orientation of magnetite should be coaxial with orientation of the *fcc* suparlattice. Therefore, these materials can be classified as mesocrystals Type I. Furthermore, by means of electron holography it was demonstrated that the magnetite particles have a flux closure magnetic vortex structure (Figure 7c,d). Based on this observation, the authors proposed that this quite unique magnetic configuration found in these nanoparticles allows the formation of colloidal crystals (mesocrystals), just before exhaustion of water from a local system within a hydrous asteroid.

2.2. Formation Principles and Fabrication Routes

Figure 8 schematically illustrates seven scenarios of different mesocrystal formation pathways: (a) alignment by organic matrix; (b) alignment by physical forces; (c) crystalline bridges, epitaxial growth and secondary nucleation; (d) alignment by spatial constraints; (e) alignment by oriented attachment; (f) alignment by face selective molecules and (g) topotactic (epitaxial) solid phase transformation. Each of these mechanisms involves different driving forces of chemical and physical origin directing the formation of the mesocrystalline materials. It is important to emphasize that depending on the formation pathway the mechanism of mesocrystal growth can be described within classical (i.e., molecule-by-molecule, ion-by-ion, etc., attachment) or non-classical (i.e., particle-by-particles attachment) crystal growth theories [11,63]. The first six of the mentioned pathways were already described in great detail (including several illustrative examples) in our recent review [34]. Therefore,

in this review we will give some examples of the formation of mesocrystals by topotactic (epitaxial) solid state transformation (Figures 8g and 9) and we will also briefly introduce techniques which can be applied for the fabrication of mesocrystals by nanopartical self-assembly (Figure 10).

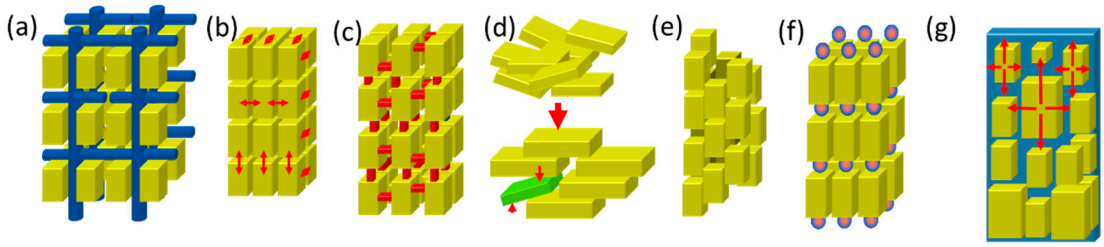

Figure 8. Simplified schematic illustration of main formation pathways of mesocrystals. (**a**) Alignment by organic matrix, (**b**) alignment by physical forces, (**c**) crystalline bridges, epitaxial growth and secondary nucleation, (**d**) alignment by spatial constraints, (**e**) alignment by oriented attachment (**f**) alignment by face selective molecules and (**g**) topotactic (epitaxial) solid phase transformation.

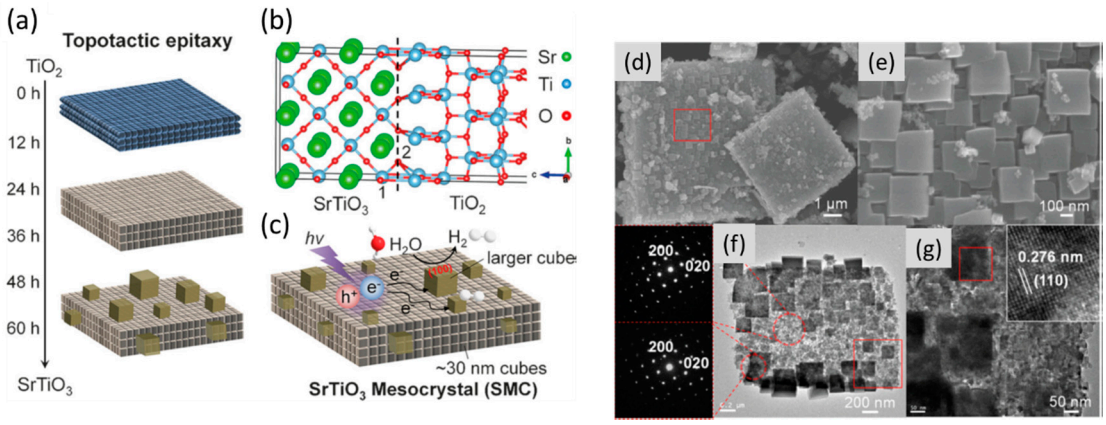

Figure 9. (**a**) Schematic illustration of the formation of $SrTiO_3$ mesocrystals (consisting of aligned nanocubes with dominant {100} facets) via topotactic epitaxial transformation of TiO_2. (**b**) Structural model of interface between $SrTiO_3$ and TiO_2 illustrating the epitaxial intergrowth of both phases. (**c**) Simplified scheme of a $SrTiO_3$ mesocrystal showing the photogeneration of electrons and holes and anisotropic electron transport from the inside to the outside. (**d**) Field emission SEM image of typical $SrTiO_3$ mesocrystals, (**e**) zoomed image inside the red frame marked in (**d**). (**f**) TEM image and corresponding ED patterns of $SrTiO_3$ mesocrystals. (**g**) High resolution TEM image of the area marked with the red-square in (**f**). Figures are adapted from Ref. [86] with permission of the Wiley-VCH Verlag GmbH & Co. KGaA, Weinheim.

The topotactic transformation in solids is well known and has been quite extensively studied for many classes of solid state materials. Based on the IUPAC (International Union of Pure and Applied Chemistry) definition, in this type of transformation "the crystal lattice of the product phase shows one or more crystallographically equivalent, orientational relationships to the crystal lattice of the parent phase" [80]. In other words, if the initial material is single crystalline (or mesocrystalline) the transformation induces the formation of a new phase in a specific crystallographic orientation. If the phase transformation starts in different parts of the initial crystal (or mesocrystal), then the resulting material will have a highly dominated mosaic structure (which might or might not transform to a single crystal at the later stages) and thus be classified as mesocrystals. Several remarkable examples of mesocrystal synthesis using this pathway have already been reported. Examples include the formation of anatase (TiO_2) from NH_4TiOF_3 [81,82], $LiCoO_2$ from $Co_2(OH)_3Cl$, $LiCoO_2$ from $Co_2(OH)_3Cl$, $LiMn_2O_4$, Li_2MnO_3, and $LiMnO_2$–Li_2MnO_3 from $MnCO_3$ [83–85], etc. Very recently,

$SrTiO_3$ mesocrystals with enhanced photocatalytic activity were produced by topotactic epitaxial transformation from anatase TiO_2 mesocrystals through a facile hydrothermal treatment (Figure 9) [86]. Due to the ordered mesocrystalline structure (Figure 9d–g) the material exhibits the three-fold photocatalytic efficiency for the hydrogen evolution reaction of water splitting in alkaline aqueous solution (Figure 9c), in comparison with conventional disordered systems.

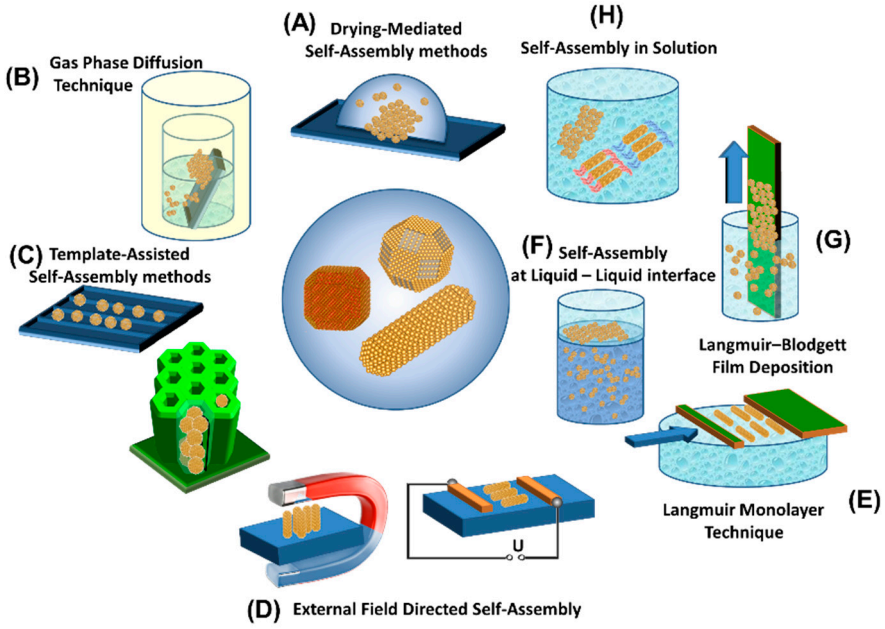

Figure 10. Schematic illustration of general methods and approaches that can be used for the fabrication of 2D and 3D nanoparticle self-assemblies (including mesocrystals).

In comparison to topotactic solid phase transformations (in which size and distribution of the building blocks in the final product are quite difficult to control) the synthesis of mesocrystals by self-assembly of nanoparticles with pre-selected composition, size and shape allows us to obtain materials with defined structure and properties [22,25,33,34,50,59,87–90]. Figure 10 illustrates different assembly techniques which can be applied to generate mesocrystals with highly ordered structures (including both translational and orientational orders of nanoparticles). Depending on the selected method, the formation of 2D and 3D mesocrystals can occur directly in solution (Figure 10b,h), on a substrate surface (Figure 10a–c,g) or at a phase interface (Figure 10e,f). Furthermore, an external magnetic and electric field can be used to direct the self-assembly processes of magnetic and/or polar nanocrystals (Figure 10d). Thus, the variation of experimental and nanoparticle variables (i.e., size, shape, surface structure, capping agent, temperature, solvent, etc.) allows for the generation of mesocrystalline materials with controllable structure and properties, which is essential, not only for fundamental science, but also in the field of application.

3. Future Outlook in Mesocrystal Research and Developments

The above few examples already demonstrate the tremendous potential of mesocrystals. Therefore, without doubt, application-driven research will be intensified and more applications will be reported. The major future developments will be twofold. New mesocrystal applications will be investigated and already existing applications improved. At the same time, though, developments in analytical techniques namely in-situ techniques like AFM, TEM and High Resolution (HR)-TEM or other in-situ microscopic and diffraction techniques, namely SAXS/WAXS, Grazing-Incidence Small-Angle Scattering (GISAXS)/ Grazing-Incidence Wide-Angle Scattering (GIWAXS), will allow for the observation of the mechanisms of mesocrystal formation, and understanding of their structuration

principles, in much more detail than it was possible before. Introduction of new methodological approaches of characterization and interpretation of mesocrystal structures, as well as defining structuration principles, will certainly allow for a deeper mechanistic understanding and the development of a theoretical description and understanding of mesocrystal formation and structure. Such theory is highly desired, since it would allow the prediction of the experimental outcome upon changes of experimental variables. Currently, a large part of optimization of mesocrystal formation reactions is done by trial and error so that a theoretical framework would largely catalyze optimization of mesocrystal formation reactions. This is particularly of importance if one thinks of the industrial application of mesocrystal systems, which is as of yet out of reach, since many mesocrystals are formed under hydrothermal conditions with long ripening times, or at room temperature in organic solvents by very slow evaporation, or in-diffusion of a non-solvent under quiescent conditions. What is needed are fast and easily controllable self-assembly mechanisms, which ideally work at room temperature. These are still missing and although Nature has shown the way of mesocrystal synthesis under such conditions, the formation strategy of mesocrystalline Biominerals is by no way fast enough for industrial demands. Therefore, either specialized and very selective and cheap organic additives need to be designed, which drive mesocrystal formation—ideally for many different systems—or a different strategy has to be designed working with many different tanks allowing for long ripening times.

To answer the question of where future applications are expected, it is helpful to take a look where mesocrystals are currently applied. One application area of current interest is the application of mesocrystals as electrodes in Li-ion batteries [45]. The mesocrystalline electrodes can provide the stability of microsized electrodes combined with the required large reactive surface of nanoparticles. So far reported mesocrystal anode materials are TiO_2, SnO_2, CuO and Fe_2O_3 with a focus on TiO_2. Cathode materials are VO_2, V_2O_5, $LiMn_2O_4$, $LiMn_{1.5}Ni_{0.5}O_4$, $LiFePO_4$. Mesocrystals are very suitable in this area because of the crystalline nature of the nanobuilding blocks and the nanocrystal orientation eliminating grain boundaries combined with the high porosity leading to a better charge and mass transport. Increasing the porosity even further while simultaneously decreasing the nanoparticle size is a goal in this area and considering the huge interest in battery technology, application of mesocrystals as electrode materials in Li-ion batteries will certainly be an important future application.

For the same reasons as stated above for electrode materials, mesocrystals are very good for applications as catalysts or sensors. As an example, for catalytic applications a particular advantage is the possibility to expose high energy surfaces like {001} of TiO_2, which are especially catalytically active. This will certainly be a goal of future research in this field, in addition to the increase of porosity and decrease of the nanoparticle size. All of the aforementioned applications require a good mass transport and therefore, a high porosity. This calls for mesocrystal synthesis routes, which do not apply organic additives, and which are not only costly, but can also block the pores for mass transport after mesocrystal assembly, so that in extreme cases, the pores are not even accessible anymore by small molecules like N_2. Due to the importance of the named materials, certainly research effort is necessary for the improvement of additive-free mesocrystal synthesis routes.

In other very promising areas, mesocrystals have not found application so far, like solar cells. For example, quantum dot based solar cells could take advantage of the special optical and electronic size-based quantum dot properties and simultaneously profit from charge transfer properties similar to those in single crystals. Or in dye sensitized solar cells, the large surface area would be beneficial for the electron transport. Therefore, research activities in these highly important areas can be expected.

Also, for plasmonic materials, the two different surface plasmon resonance bands for metal nanorods can lead to interesting directional couplings in metal nanoparticle mesocrystals, and therefore, further exploitation of metal nanoparticle mesocrystals can be foreseen for the future. A similar application range can be foreseen for mesocrystals from magnetic nanoparticles where coupling of the magnetic fields can be exploited. For example, linear arrangement of magnetite nanoparticles leads to coupling of their magnetic fields in a way that they magnetically behave like a single rod-shaped magnet with high magnetic field strength (Figure 6 blue frame).

Considering the medical field, mesocrystals are also underrepresented. If one keeps in mind that bone or dentin in teeth show a mesocrystalline arrangement of the hydroxyapatite platelets on the lowest hierarchical tier, application of mesocrystals in medical applications related to bone or teeth can be expected. For example, mesocrystalline bone implants would mimic the natural bone structure as closely as possible. The same is true for dentine in teeth. Besides these applications, a huge potential of mesocrystals is seen in pharmaceutical formulations. If drugs with a mesocrystal structure can be realized, their dissolution kinetics can be enhanced significantly since the advantageous solubility of nanoparticles can be combined with micro/macroscopic particles which can be easily handled with existing technology. A first demonstration was reported for Ibuprofen [91].

Taking the lessons from biomineralization, mesocrystal structures should also be very promising in building materials. Their mechanical properties can certainly be much enhanced by a layered organic–inorganic structure. However, the synthesis of mesocrystals might be too costly in this application area and perhaps, the required mass production of mesocrystalline building materials is also not possible to the required extent.

What is essentially, up to now, an untouched area in mesocrystal research, is mesocrystals of organic nanocrystals; although, alanine [92], lysine [93], perylentetetracarboxylate [94] and ibuprofen [91] were reported as very first examples to form mesocrystals. The potential in pharmaceutical formulations was already mentioned above and this concerns organic nanocrystals. However, the example of perylenetetracarboxylate as a n-type semiconductor demonstrates that optical and electronic properties can also be influenced by the mesocrystal structure so that future potential for mesocrystalline structures is also seen in organic electronics and optoelectronic applications.

Besides the aforementioned "classical" mesocrystalline structures which mainly rely on the arrangement of a single nanocrystal species, one can also envision hybrid structures. For example, conducting materials like graphene or metal nanowires or conducting polymers could be used as building/spacer units in the mesocrystal formation besides the nanocrystals, and in that way, allow for the fabrication of nanoelectronic devices.

Also, if not only one nanocrystalline species is applied for mesocrystal formation, but two or more, the properties of these nanocrystals can be combined leading to new and emergent properties. For example, quantum dots with a fluorescence at the wavelength of the plasmon resonance of a metal nanoparticle could compensate for the energy loss due to light absorption by the metal nanoparticle. Also the combination of magnetic and metallic nanoparticles might lead to interesting properties. Or more generally, nanoparticles with disparate properties could be combined, leading to combinations like hard—soft or conductor—isolators, which could lead to mechanically improved materials or materials with outstanding electrical properties like super capacitors. The potential of such mesocrystalline structures is tremendous, but such combination is by no means easy. It relies on nanoparticles with the same size or shape or at least compatible sizes and shapes which can be self-assembled to ordered structures. In addition, the surface chemistry of the nanoparticles needs to be compatible either in the form of the same stabilizer like oleic acid, for example, or the same kind of charge stabilization. Furthermore, even if such binary mesocrystal systems assemble, it is not yet clear if the two nanoparticle species will randomly mix, or will form highly ordered new supperlattices, or if domains of the same nanoparticles will be assembled. Despite the already foreseeable difficulties, such multiparticle systems have great potential for mesocrystals toward a toolbox for tailored mesocrystal properties.

In summary, the focused and systematic research on mesocrystals (which are a special type of nanostructured materials) only started about 10 years ago, but already now, mesocrystalline materials with outstanding properties, or even otherwise unreachable properties for the bulk material under consideration are available. However, the greatest obstacle for a targeted fabrication is the so far insufficient understanding of mesocrystal formation mechanisms, structuration principles and the lack of a theoretical description. Mesocrystals are still a challenge for analytics and the progress in analytical equipment development will hopefully help to solve the open questions related to

mesocrystal formation, structure and properties. On the application side, the potential has already become obvious, and due to the advantages of mesocrystals in energy related or catalysis applications, a lot of research activity and progress can be expected in this globally important area. However, the application range of mesocrystals is by far broader than what is currently known. Therefore, a lot of exciting developments can be expected in the field of mesocrystals—we are very curious about what will emerge.

Acknowledgments: The authors thank the DFG (Deutsche Forschungsgemeinschaft) for the support of this work within the SFB 1214. They also thank Rudiger Kniep, Paul Simon, Igor A. Baburin, L. Bergström, A. Shtukenberg, S. Sturm for useful discussions. Elena V. Sturm additionally acknowledges a fellowship of the Zukunftskolleg of the University of Konstanz.

Conflicts of Interest: The authors declare no conflict of interest.

References

1. Cölfen, H.; Mann, S. Higher-order organization by mesoscale self-assembly and transformation of hybrid nanostructures. *Angew. Chem. Int. Edit.* **2003**, *42*, 2350–2365. [CrossRef] [PubMed]
2. Cölfen, H.; Antonietti, M. Mesocrystals: Inorganic superstructures made by highly parallel crystallization and controlled alignment. *Angew. Chem. Int. Edit.* **2005**, *44*, 5576–5591. [CrossRef] [PubMed]
3. Niederberger, M.; Cölfen, H. Oriented attachment and mesocrystals: Non-classical crystallization mechanisms based on nanoparticle assembly. *Phys. Chem. Chem. Phys.* **2006**, *8*, 3271–3287. [CrossRef] [PubMed]
4. Cölfen, H.; Antonietti, M. *Mesocrystals and Nonclassical Crystallization*; John Wiley & Sons: Chichester, UK, 2008.
5. Canaveras, J.C.; SanchezMoral, S.; Calvo, J.P.; Hoyos, M.; Ordonez, S. Dedolomites associated with karstification. An example of early dedolomitization in lacustrine sequences from the tertiary madrid basin, central spain. *Carbonates Evaporites* **1996**, *11*, 85–103. [CrossRef]
6. Depmeier, W. Mesocrystallography. *Ann. Chim. Sci. Mat.* **1998**, *23*, 43–48. [CrossRef]
7. Hartley, A.J.; May, G. Miocene gypcretes from the calama basin, northern chile. *Sedimentology* **1998**, *45*, 351–364. [CrossRef]
8. Ko, C.H.; Kim, J.M.; Ryoo, R. Mesocrystal engineering using non-bonded interaction to obtain optically transparent mesoporous silica films and plates with uniform orientation. *Microporous Mesoporous Mat.* **1998**, *21*, 235–243. [CrossRef]
9. Yamada, K.; Kohiki, S. Dielectric and optical properties of batio3 mesocrystals. *Physica E* **1999**, *4*, 228–230. [CrossRef]
10. Schaskolsky, M.; Schubnikow, A. On the synthesis of regular crystal intergrowths of potassium alum. *Zeitschrift Fur Kristallographie* **1933**, *85*, 1–16.
11. Chernov, A.A. *Modern Crystallography: Crystal Growth*, 1st ed.; Springer-Verlag: Berlin/Heidelberg, Germany, 1984; Volume 3.
12. Ivanov, V.K.; Fedorov, P.P.; Baranchikov, A.Y.; Osiko, V.V. Oriented attachment of particles: 100 Years of investigations of non-classical crystal growth. *Russ. Chem. Rev.* **2014**, *83*, 1204–1222. [CrossRef]
13. Shubnikov, A.V. *Kak rastut kristally*; Academy of Sciences of the USSR: Moscow, Russia, 1935.
14. Yishkin, N.P. *Teoriya Mikroblochnogo Rosta Kristallov v Priridnykh Geotermicheskikh Rastvorakh*; Institute of Geology, Komi Branch of Academy of Science of the USSR: Syktyvkar, Russia, 1971.
15. Melikhov, I.V.; Mikheeva, I.E.; Rudin, V.N. Directional aggregation in highly dispersed suspensions. *Colloid J. USSR* **1988**, *50*, 755–760.
16. Melikhov, I.V.; Mikheeva, I.E.; Rudin, V.N. On the possibility of block crystal-growth of calcium-sulfate semihydrate from high supersaturation solutions. *Kristallografiya* **1989**, *34*, 1272–1278.
17. Kuleshova, O.V. *Elementarnye Akty Kristallizacii Polugidrata Sulfata Kalciya iz Rastvorov*; Lomonosov Moscow State University, Rotoprint PKB CT MPS: Moscow, Russia, 1991; p. 128.
18. Vainshtein, B.K. Modern crystallography. Vol. 1. Fundamentals of crystals. Symmetry, and methods of structural crystallography. *Acta Cryst.* **1995**, *51*, 234–235.

19. Melikhov, I.V.; Kitova, E.N.; Kamenskaya, A.N.; Kozlovskaya, E.D.; Mikheev, N.B.; Kulyukhin, S.A. Monocrystallomimicry in the aerosols of ammonium and cesium halogenides. *Kolloidnyj Zhurnal* **1997**, *59*, 723–728.
20. Uyeda, N. *Substructures of Colloidal Silver Particles*; Institute for Chemical Research, Kyoto University: Kyoto, Japan, 1969; Volume 47, pp. 426–436.
21. Efremov, I.F. *Periodicheskie Kolloidnye Struktury*; Khimia: Leninigrad, Russia, 1971; p. 192.
22. Quan, Z.; Fang, J. Superlattices with non-spherical building blocks. *Nano Today* **2010**, *5*, 390–411. [CrossRef]
23. Vanmaekelbergh, D. Self-assembly of colloidal nanocrystals as route to novel classes of nanostructured materials. *Nano Today* **2011**, *6*, 419–437. [CrossRef]
24. Kovalenko, M.V.; Manna, L.; Cabot, A.; Hens, Z.; Talapin, D.V.; Kagan, C.R.; Klimov, V.I.; Rogach, A.L.; Reiss, P.; Milliron, D.J.; et al. Prospects of nanoscience with nanocrystals. *ACS Nano* **2015**, *9*, 1012–1057. [CrossRef] [PubMed]
25. Boles, M.A.; Engel, M.; Talapin, D.V. Self-assembly of colloidal nanocrystals: From intricate structures to functional materials. *Chem. Rev.* **2016**, *116*, 11220–11289. [CrossRef] [PubMed]
26. Blüh, O. Einige bei der Untersuchung von Kolloiden im Wechselfeld auftretende Erscheinungen. *Kolloid-Zeitschrift* **1925**, *37*, 267–270. [CrossRef]
27. Zocher, H. On independent structure formation in brine. *Z. Anorg. Allg. Chem.* **1925**, *147*, 91–110. [CrossRef]
28. Zocher, H.; Heller, W. Schiller layers as reaction products of slow iron chloride-hydrolysis. *Z. Anorg. Allg. Chem.* **1929**, *186*, 75–96. [CrossRef]
29. Heller, W.; Zocher, H. Cross-line magneto-optical anisotropy of some colloidal solutions. II. Iron oxide. (a summarising overview.). *Zeitschrift für Physikalische Chemie-Abteilung a-Chemische Thermodynamik Kinetik Elektrochemie Eigenschaftslehre* **1933**, *166*, 365–381.
30. Heller, W. Physical chemistry—Distances between the colloidal particles in the bright layers of certain iron oxide soils. *Comptes Rendus Hebdomadaires Des Seances De L Academie Des Sciences* **1935**, *201*, 831–833.
31. Watson, J.H.L.; Heller, W.; Cardell, R.R. Internal structure of colloidal crystals of beta-feooh and remarks on their assemblies in schiller layers. *J. Phys. Chem.* **1962**, *66*, 1757–1763. [CrossRef]
32. Distler, G.I.; Borisova, N.M. Elektronno-mikroskopicheskie issledovaniya aktivnyh zentrov poverhnostey tverdyh tel. *Kinetika i Kataliz* **1967**, *8*, 944.
33. Bergstrom, L.; Sturm, E.V.; Salazar-Alvarez, G.; Cölfen, H. Mesocrystals in biominerals and colloidal arrays. *Acc. Chem. Res.* **2015**, *48*, 1391–1402. [CrossRef] [PubMed]
34. Sturm, E.V.; Cölfen, H. Mesocrystals: Structural and morphogenetic aspects. *Chem. Soc. Rev.* **2016**, *45*, 5821–5833. [CrossRef] [PubMed]
35. Seto, J.; Ma, Y.R.; Davis, S.A.; Meldrum, F.; Gourrier, A.; Kim, Y.Y.; Schilde, U.; Sztucki, M.; Burghammer, M.; Maltsev, S.; et al. Structure-property relationships of a biological mesocrystal in the adult sea urchin spine. *Proc. Natl. Acad. Sci. USA* **2012**, *109*, 3699–3704. [CrossRef] [PubMed]
36. Li, X.D.; Xu, Z.H.; Wang, R.Z. In situ observation of nanograin rotation and deformation in nacre. *Nano Lett.* **2006**, *6*, 2301–2304. [CrossRef] [PubMed]
37. Perrin, J.; Vielzeuf, D.; Ricolleau, A.; Dallaporta, H.; Valton, S.; Floquet, N. Block-by-block and layer-by-layer growth modes in coral skeletons. *Am. Miner.* **2015**, *100*, 681–695. [CrossRef]
38. Vielzeuf, D.; Floquet, N.; Chatain, D.; Bonneté, F.; Ferry, D.; Garrabou, J.; Stolper, E.M. Multilevel modular mesocrystalline organization in red coral. *Am. Miner.* **2010**, *95*, 242–248. [CrossRef]
39. Vielzeuf, D.; Garrabou, J.; Baronnet, A.; Grauby, O.; Marschal, C. Nano to macroscale biomineral architecture of red coral. *Am. Miner.* **2008**, *93*, 1799–1815. [CrossRef]
40. Floquet, N.; Vielzeuf, D. Ordered misorientations and preferential directions of growth in mesocrystalline red coral sclerites. *Cryst. Growth Des.* **2012**, *12*, 4805–4820. [CrossRef]
41. Oaki, Y.; Kotachi, A.; Miura, T.; Imai, H. Bridged nanocrystals in biominerals and their biomimetics: Classical yet modern crystal growth on the nanoscale. *Adv. Funct. Mater.* **2006**, *16*, 1633–1639. [CrossRef]
42. Cai, J.G.; Qi, L.M. Tio2 mesocrystals: Synthesis, formation mechanisms and applications. *Sci. China Chem.* **2012**, *55*, 2318–2326. [CrossRef]
43. Ma, M.G.; Cölfen, H. Mesocrystals–applications and potential. *Curr. Opin. Colloid Interface Sci.* **2014**, *19*, 56–65. [CrossRef]
44. Tachikawa, T.; Majima, T. Metal oxide mesocrystals with tailored structures and properties for energy conversion and storage applications. *NPG Asia Mate.* **2014**, *6*, e100. [CrossRef]

45. Uchaker, E.; Cao, G.Z. Mesocrystals as electrode materials for lithium-ion batteries. *Nano Today* **2014**, *9*, 499–524. [CrossRef]
46. Haberkorn, H.; Franke, D.; Frechen, T.; Goesele, W.; Rieger, J. Early stages of particle formation in precipitation reactions—Quinacridone and boehmite as generic examples. *J. Colloid Interface Sci.* **2003**, *259*, 112–126. [CrossRef]
47. Pontoni, D.; Bolze, J.; Dingenouts, N.; Narayanan, T.; Ballauff, M. Crystallization of calcium carbonate observed in-situ by combined small- and wide-angle x-ray scattering. *J. Phys. Chem. B* **2003**, *107*, 5123–5125. [CrossRef]
48. Thomas, J.M.; Simpson, E.T.; Kasama, T.; Dunin-Borkowski, R.E. Electron holography for the study of magnetic nanomaterials. *Acc. Chem. Res.* **2008**, *41*, 665–674. [CrossRef] [PubMed]
49. Kimura, Y.; Sato, T.; Nakamura, N.; Nozawa, J.; Nakamura, T.; Tsukamoto, K.; Yamamoto, K. Vortex magnetic structure in framboidal magnetite reveals existence of water droplets in an ancient asteroid. *Nat. Commun.* **2013**, *4*, 2649. [CrossRef] [PubMed]
50. Brunner, J.; Baburin, I.A.; Sturm, S.; Kvashnina, K.; Rossberg, A.; Pietsch, T.; Andreev, S.; Sturm, E.; Cölfen, H. Self-assembled magnetite mesocrystalline films: Toward structural evolution from 2D to 3D superlattices. *Adv. Mater. Interfaces* **2017**, *4*, 1600431. [CrossRef]
51. Kniep, R.; Simon, P.; Rosseeva, E. Structural complexity of hexagonal prismatic crystal specimens of fluorapatite-gelatine nanocomposites: A case study in biomimetic crystal research. *Cryst. Res. Technol.* **2014**, *49*, 4–13. [CrossRef]
52. Kniep, R.; Simon, P. Fluorapatite-gelatine-nanocomposites: Self-organized morphogenesis, real structure and relations to natural hard materials. In *Biomineralization I: Crystallization and Self-Organization Process*; Naka, K., Ed.; Springer-Verlag: Berlin/Heidelberg, Germany, 2007; Volume 270, pp. 73–125.
53. Natalio, F.; Corrales, T.P.; Panthoefer, M.; Schollmeyer, D.; Lieberwirth, I.; Mueller, W.E.G.; Kappl, M.; Butt, H.-J.; Tremel, W. Flexible minerals: Self-assembled calcite spicules with extreme bending strength. *Science* **2013**, *339*, 1298–1302. [CrossRef] [PubMed]
54. Zhou, L.; O'Brien, P. Mesocrystals: A new class of solid materials. *Small* **2008**, *4*, 1566–1574. [CrossRef] [PubMed]
55. Song, R.Q.; Cölfen, H. Mesocrystals-ordered nanoparticle superstructures. *Adv. Mater.* **2010**, *22*, 1301–1330. [CrossRef] [PubMed]
56. Fang, J.X.; Ding, B.J.; Gleiter, H. Mesocrystals: Syntheses in metals and applications. *Chem. Soc. Rev.* **2011**, *40*, 5347–5360. [CrossRef] [PubMed]
57. Zhou, L.; O'Brien, P. Mesocrystals—Properties and applications. *J. Phys. Chem. Lett.* **2012**, *3*, 620–628. [CrossRef] [PubMed]
58. Cölfen, H. Polymer-mediated growth of crystals and mesocrystals. In *Research Methods in Biomineralization Science*, 1st ed.; Yoreo, J.J.D., Ed.; Elsevier: Amsterdam, The Netherlands, 2013; Volume 532, pp. 277–304.
59. Bahrig, L.; Hickey, S.G.; Eychmuller, A. Mesocrystalline materials and the involvement of oriented attachment—A review. *CrystEngComm* **2014**, *16*, 9408–9424. [CrossRef]
60. Bu, F.X.; Du, C.J.; Jiang, J.S. Synthesis, properties and applications of mesocrystals. *Prog. Chem.* **2014**, *26*, 75–86.
61. Simon, P.; Bahrig, L.; Baburin, I.A.; Formanek, P.; Roeder, F.; Sickmann, J.; Hickey, S.G.; Eychmueller, A.; Lichte, H.; Kniep, R.; et al. Interconnection of nanoparticles within 2D superlattices of PbS/oleic acid thin films. *Adv. Mater.* **2014**, *26*, 3042–3049. [CrossRef] [PubMed]
62. Simon, P.; Rosseeva, E.; Baburin, I.A.; Liebscher, L.; Hickey, S.G.; Cardoso-Gil, R.; Eychmüller, A.; Kniep, R.; Carrillo-Cabrera, W. PbS–organic mesocrystals: The relationship between nanocrystal orientation and superlattice array. *Angew. Chem. Int. Ed.* **2012**, *51*, 10776–10781. [CrossRef] [PubMed]
63. De Yoreo, J.J.; Gilbert, P.; Sommerdijk, N.; Penn, R.L.; Whitelam, S.; Joester, D.; Zhang, H.Z.; Rimer, J.D.; Navrotsky, A.; Banfield, J.F.; et al. Crystallization by particle attachment in synthetic, biogenic, and geologic environments. *Science* **2015**, *349*, aaa6760. [CrossRef] [PubMed]
64. Li, D.S.; Nielsen, M.H.; Lee, J.R.I.; Frandsen, C.; Banfield, J.F.; De Yoreo, J.J. Direction-specific interactions control crystal growth by oriented attachment. *Science* **2012**, *336*, 1014–1018. [CrossRef] [PubMed]
65. De Yoreo, J.J. In-situ liquid phase tem observations of nucleation and growth processes. *Prog. Cryst. Growth Charact. Mater.* **2016**, *62*, 69–88. [CrossRef]

66. Li, R.; Bian, K.; Hanrath, T.; Bassett, W.A.; Wang, Z. Decoding the superlattice and interface structure of truncate PbS nanocrystal-assembled supercrystal and associated interaction forces. *J. Am. Chem. Soc.* **2014**, *136*, 12047–12055. [CrossRef] [PubMed]
67. Li, R.; Bian, K.; Wang, Y.; Xu, H.; Hollingsworth, J.A.; Hanrath, T.; Fang, J.; Wang, Z. An obtuse rhombohedral superlattice assembled by Pt nanocubes. *Nano Lett.* **2015**, *15*, 6254–6260. [CrossRef] [PubMed]
68. Li, R.; Zhang, J.; Tan, R.; Gerdes, F.; Luo, Z.; Xu, H.; Hollingsworth, J.A.; Klinke, C.; Chen, O.; Wang, Z. Competing interactions between various entropic forces toward assembly of Pt_3Ni octahedra into a body-centered cubic superlattice. *Nano Lett.* **2016**, *16*, 2792–2799. [CrossRef] [PubMed]
69. Zhang, J.; Zhu, J.L.; Li, R.P.; Fang, J.Y.; Wang, Z.W. Entropy-driven Pt_3Co nanocube assembles and thermally mediated electrical conductivity with anisotropic variation of the rhombohedral superlattice. *Nano Lett.* **2017**, *17*, 362–367. [CrossRef] [PubMed]
70. Agthe, M.; Hoydalsvik, K.; Mayence, A.; Karvinen, P.; Liebi, M.; Bergstrom, L.; Nygard, K. Controlling orientational and translational order of iron oxide nanocubes by assembly in nanofluidic containers. *Langmuir* **2015**, *31*, 12537–12543. [CrossRef] [PubMed]
71. Agthe, M.; Plivelic, T.S.; Labrador, A.; Bergström, L.; Salazar-Alvarez, G. Following in real time the two-step assembly of nanoparticles into mesocrystals in levitating drops. *Nano Lett.* **2016**, *16*, 6838–6843. [CrossRef] [PubMed]
72. Agthe, M.; Wetterskog, E.; Mouzon, J.; Salazar-Alvarez, G.; Bergstrom, L. Dynamic growth modes of ordered arrays and mesocrystals during drop-casting of iron oxide nanocubes. *Crystengcomm* **2014**, *16*, 1443–1450. [CrossRef]
73. Disch, S.; Wetterskog, E.; Hermann, R.P.; Salazar-Alvarez, G.; Busch, P.; Brueckel, T.; Bergstroem, L.; Kamali, S. Shape induced symmetry in self-assembled mesocrystals of iron oxide nanocubes. *Nano Lett.* **2011**, *11*, 1651–1656. [CrossRef] [PubMed]
74. Faure, B.; Wetterskog, E.; Gunnarsson, K.; Josten, E.; Hermann, R.P.; Brueckel, T.; Andreasen, J.W.; Meneau, F.; Meyer, M.; Lyubartsev, A.; et al. 2D to 3D crossover of the magnetic properties in ordered arrays of iron oxide nanocrystals. *Nanoscale* **2013**, *5*, 953–960. [CrossRef] [PubMed]
75. Wetterskog, E.; Klapper, A.; Disch, S.; Josten, E.; Hermann, R.P.; Rucker, U.; Bruckel, T.; Bergstrom, L.; Salazar-Alvarez, G. Tuning the structure and habit of iron oxide mesocrystals. *Nanoscale* **2016**, *8*, 15571–15580. [CrossRef] [PubMed]
76. Weidman, M.C.; Smilgies, D.M.; Tisdale, W.A. Kinetics of the self-assembly of nanocrystal superlattices measured by real-time in situ x-ray scattering. *Nat. Mater.* **2016**, *15*, 775–781. [CrossRef] [PubMed]
77. Dunin-Borkowski, R.E.; McCartney, M.R.; Frankel, R.B.; Bazylinski, D.A.; Posfai, M.; Buseck, P.R. Magnetic microstructure of magnetotactic bacteria by electron holography. *Science* **1998**, *282*, 1868–1870. [CrossRef] [PubMed]
78. Ohfuji, H.; Boyle, A.P.; Prior, D.J.; Rickard, D. Structure of framboidal pyrite: An electron backscatter diffraction study. *Am. Miner.* **2005**, *90*, 1693–1704. [CrossRef]
79. Ohfuji, H.; Rickard, D. Experimental syntheses of framboids—A review. *Earth Sci. Rev.* **2005**, *71*, 147–170. [CrossRef]
80. McNaught, A.D.; McNaught, A.D. *Compendium of Chemical Terminology*, 2nd ed.; Blackwell Scientific Publications: Oxford, UK, 1997; Volume 1669.
81. Zhou, L.; Boyle, D.S.; O'Brien, P. Uniform NH_4TiOF_3 mesocrystals prepared by an ambient temperature self-assembly process and their topotaxial conversion to anatase. *Chem. Commun.* **2007**, *2*, 144–146. [CrossRef] [PubMed]
82. Zhou, L.; Smyth-Boyle, D.; O'Brien, P. A facile synthesis of uniform nh4tiof3 mesocrystals and their conversion to TiO_2 mesocrystals. *J. Am. Chem. Soc.* **2008**, *130*, 1309–1320. [CrossRef] [PubMed]
83. Dang, F.; Hoshino, T.; Oaki, Y.; Hosono, E.; Zhou, H.; Imai, H. Synthesis of Li-Mn-O mesocrystals with controlled crystal phases through topotactic transformation of $MnCO_3$. *Nanoscale* **2013**, *5*, 2352–2357. [CrossRef] [PubMed]
84. Imai, H. Mesostructured crystals: Growth processes and features. *Prog. Cryst. Growth Charact. Mater.* **2016**, *62*, 212–226. [CrossRef]
85. Nakajima, K.; Oaki, Y.; Imai, H. Syntheses of $LiCoO_2$ mesocrystals by topotactic transformation and their electrochemical properties. *ChemPlusChem* **2013**, *78*, 1379–1383. [CrossRef]

86. Zhang, P.; Ochi, T.; Fujitsuka, M.; Kobori, Y.; Majima, T.; Tachikawa, T. Topotactic epitaxy of $SrTiO_3$ mesocrystal superstructures with anisotropic construction for efficient overall water splitting. *Angew. Chem. Int. Edit.* **2017**, *56*, 5299–5303. [CrossRef] [PubMed]
87. Hanrath, T. Colloidal nanocrystal quantum dot assemblies as artificial solids. *J. Vac. Sci. Technol. A* **2012**, *30*, 030802. [CrossRef]
88. Kato, K.; Mimura, K.; Dang, F.; Imai, H.; Wada, S.; Osada, M.; Haneda, H.; Kuwabara, M. $BaTiO_3$ nanocube and assembly to ferroelectric supracrystals. *J. Mater. Res.* **2013**, *28*, 2932–2945. [CrossRef]
89. Zhang, S.Y.; Regulacio, M.D.; Han, M.Y. Self-assembly of colloidal one-dimensional nanocrystals. *Chem. Soc. Rev.* **2014**, *43*, 2301–2323. [CrossRef] [PubMed]
90. Talapin, D.V.; Shevchenko, E.V. Introduction: Nanoparticle chemistry. *Chem. Rev.* **2016**, *116*, 10343–10345. [CrossRef] [PubMed]
91. Lee, T.; Zhang, C.W. Dissolution enhancement by bio-inspired mesocrystals: The study of racemic (R,S)-(+/−)-sodium ibuprofen dihydrate. *Pharm. Res.* **2008**, *25*, 1563–1571. [CrossRef] [PubMed]
92. Wohlrab, S.; Pinna, N.; Antonietti, M.; Cölfen, H. Polymer-induced alignment of DL-alanine nanocrystals to crystalline mesostructures. *Chem. Eur. J.* **2005**, *11*, 2903–2913. [CrossRef] [PubMed]
93. Jiang, Y.; Gong, H.F.; Grzywa, M.; Volkmer, D.; Gower, L.; Cölfen, H. Microdomain transformations in mosaic mesocrystal thin films. *Adv. Funct. Mater.* **2013**, *23*, 1547–1555. [CrossRef]
94. Huang, M.; Schilde, U.; Kumke, M.; Antonietti, M.; Cölfen, H. Polymer-induced self-assembly of small organic molecules into ultralong microbelts with electronic conductivity. *J. Am. Chem. Soc.* **2010**, *132*, 3700–3707. [CrossRef] [PubMed]